Electronic Supplementary Material (ESI) for Catalysis Science & Technology.

Supplementary data

Adjusting matched-degree between electron library and surface-active sites and forming surface polarization in MOF-based photo-cocatalyst for accelerating electron transfer

Ling Ding[a], Qianqian Sun[a], Zebin Yu*[a], Lei Sun*[b], Ronghua Jiang[c], Yanping Hou[a], Jun Huang[d], Tao Zhong[a], Huajiao Chen[a], CuiFang Lian[a], Ben Fan[a]

[a] MOE Key Laboratory of New Processing Technology for Norferrous Metals and Materials, Guangxi key Laboratory of Processing for Norferrous Featured Metals and Materials, School of Resources, Environment and Materials, Nanning 530004 Guangxi, P.R.China.

[b] School of Chemical Engineering and Technology, Hainan University, Haikou 570228, PR China

[c] School of Chemical and Environmental Engineering, Shaoguan University, Shaoguan 512005, P. R. China.

[d]College of Civil Engineering & Architecture, Guangxi University, Nanning 530004, P. R. China

* Corresponding author.

Tel.: + 8613877108420 (Z. Yu)

E-mail: xxzx7514@hotmail.com (Z. Yu), sunlei0620@163.com (L. Sun)

1. Experimental section

1.1. Characterization

In order to analyse the crystalline structures, the samples were characterized by X-ray diffraction using a Dandong Fangyuan DX-2700A X-ray diffractometer with Cu Kα radiation, ranged from 10° to 80°. The morphologies of the samples were determined with a field emission scanning electron microscopy (FESEM, Hitachi SU8020), transmission electron microscopy (TEM, FEI Talos F200X) and a high-resolution transmission electron microscopy (HRTEM). Elemental analysis of the samples was conducted by an energy dispersive X-ray spectrometer (EDS) attached to TEM. Laser Raman spectrometer (Raman, Renishaw in Via Reflex) was used to analyse the composition and structure of the materials. The chemical state of the samples was analysed by an X-ray photoelectron spectroscopy (XPS, Thermo ESCALAB 250XI). UV–visible diffuse reflectance spectra (UV-vis DRS) were measured using a Shimadzu UV-3600plus spectrometer with $BaSO_4$-coated integration sphere in the region of 220-800 nm. The Zeta potentials of the samples were measured by Zetasizer nano (Malvern Zetasizer Nano ZS90). The photoluminescence spectra for the samples were investigated on a steady-state fluorescence spectrometer (PL, OmniFluo-960) with an excitation wave length of 325 nm. A Kelvin probe apparatus (Bruker Dimension Icon) was detected the work function and surface potential (SP), And it was calibrated by the highly oriented pyrolytic graphite as a standard reference surface.

1.2. Photocatalytic activity measurement

The photocatalytic H_2 production test was carried out in an airtight quartz reactor. 40 mg of photocatalyst was dispersed into 80 mL lactic acid aqueous solution (10 vol%) by ultrasonication about 5 min. Prior to irradiation, the solution in the reactor was bubbled with N_2 for 10 min to remove the dissolved oxygen. During the reaction, the mixture was constantly stirred by a magnetic stirrer and the solution was kept at room temperature through cooling water circulation system. A 300 W Xe lamp (CEL-HXF300F3, Beijing China Education Au-light Co., Ltd., China) with a 400 nm UV-cut-off filter was used as visible light source to conduct the H_2 production reaction. 1 mL gas was regularly extracted from the photocatalytic reactor and determined by gas chromatograph (GC7920-T, China), assembled with a thermal conductivity detector (TCD) and a 5 Å molecular sieve column with N_2 as the carrier gas. The apparent quantum yield (AQY) was measured under the same photocatalytic reaction condition and irradiated by the 300 W Xe lamp with the 420 nm band-pass filter. The Xe lamp was used as the light source through a filter cutting off with an intensity of 35 W/m^2. The irradiation area is 15.19 cm^2. The AQY was calculated according to the equation below:

$$AQY = \frac{2 \times the\ number\ of\ hydrogen\ molecules}{the\ number\ of\ incident\ photons} \times 100\%$$

1.3. Photoelectrochemical measurements

All the electrochemical measurements were measured on a CHI660E electrochemical work station (Chenhua Instrument, Shanghai, China) with a standard three electrode system. The preparation method of working electrodes are as follows. 10 mg of the as-synthesized sample was dispersed into a mixed solution containing 10 μL of 5 wt % Nafion solution and 1 mL of absolute ethanol. Then, 30 μL of the slurry was dipped onto the surface of the indium tin oxide (ITO) glass substrate with an area of 1 cm × 1 cm. The saturated calomel electrode (SCE) and Pt plate were used as reference and counter electrodes, respectively. 0.5 M Na_2SO_4 solution was used as the electrolyte. Transient photocurrent measurements were carried on in an above-motioned standard three-electrode system. A 300 W Xe lamp with the UV cut-off filter was used to provide the visible light source ($\lambda \geq 400$ nm). The Electrochemical impedance spectroscopy (EIS) measurements were also carried out with the above-mentioned working electrodes in the CHI660E three-electrode system under the same conditions in dark. During the measurement, the frequency was in the range of 0.1 to 105 Hz. The Mott-Schottky plots were also recorded using the CHI660E three-electrode system at an AC frequency of 500, 1000 and 1500 Hz in 0.5 M Na_2SO_4 solution.

1.4 Density function theory (DFT) calculation details

The Density functional calculation (DFT) was performed for Ni substitution and no substitution Co using Materials studio which depends on the first principal calculation by applying the following conditions: Generalized Gradient Approximation (GGA) for the exchange-correlation function in the framework of Perdew Burke Ernzerhof (PBE). The Brillourin zone was sampled with Monkhorst mesh 2× 4 × 2 through all the computational process. The energy cutoff was set to 400 eV. The convergence threshold for self-consistent calculations was $2.0e^{-6}$ eV per atom and the force on each atom less than 0.05 eV/Å was set for convergence criterion of geometry relaxation.

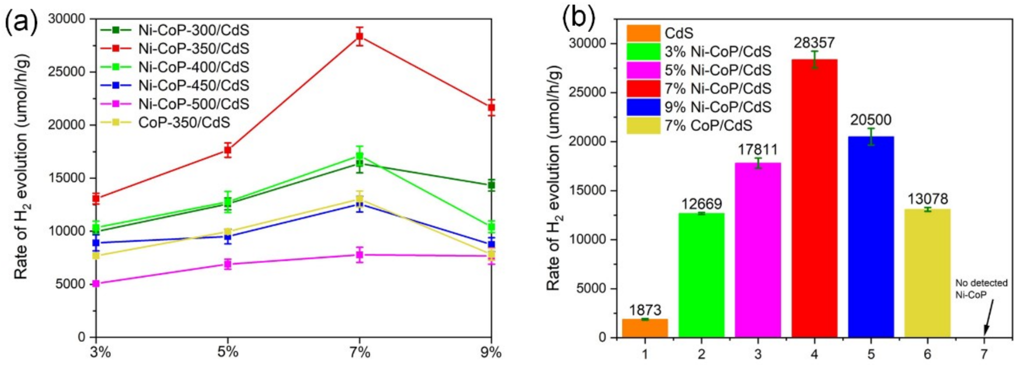

Fig. S1. (a) Comparison of PHP rate at different temperatures and loading amount. (b) Comparison of photocatalytic H_2 production rates in different samples.

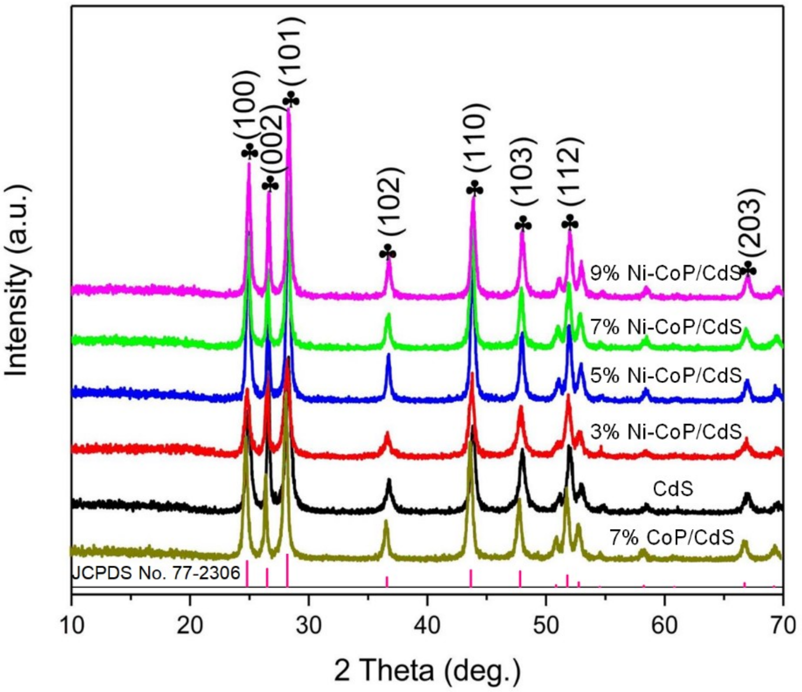

Fig. S2. XRD patterns of the CdS and the composite photocatalysts.

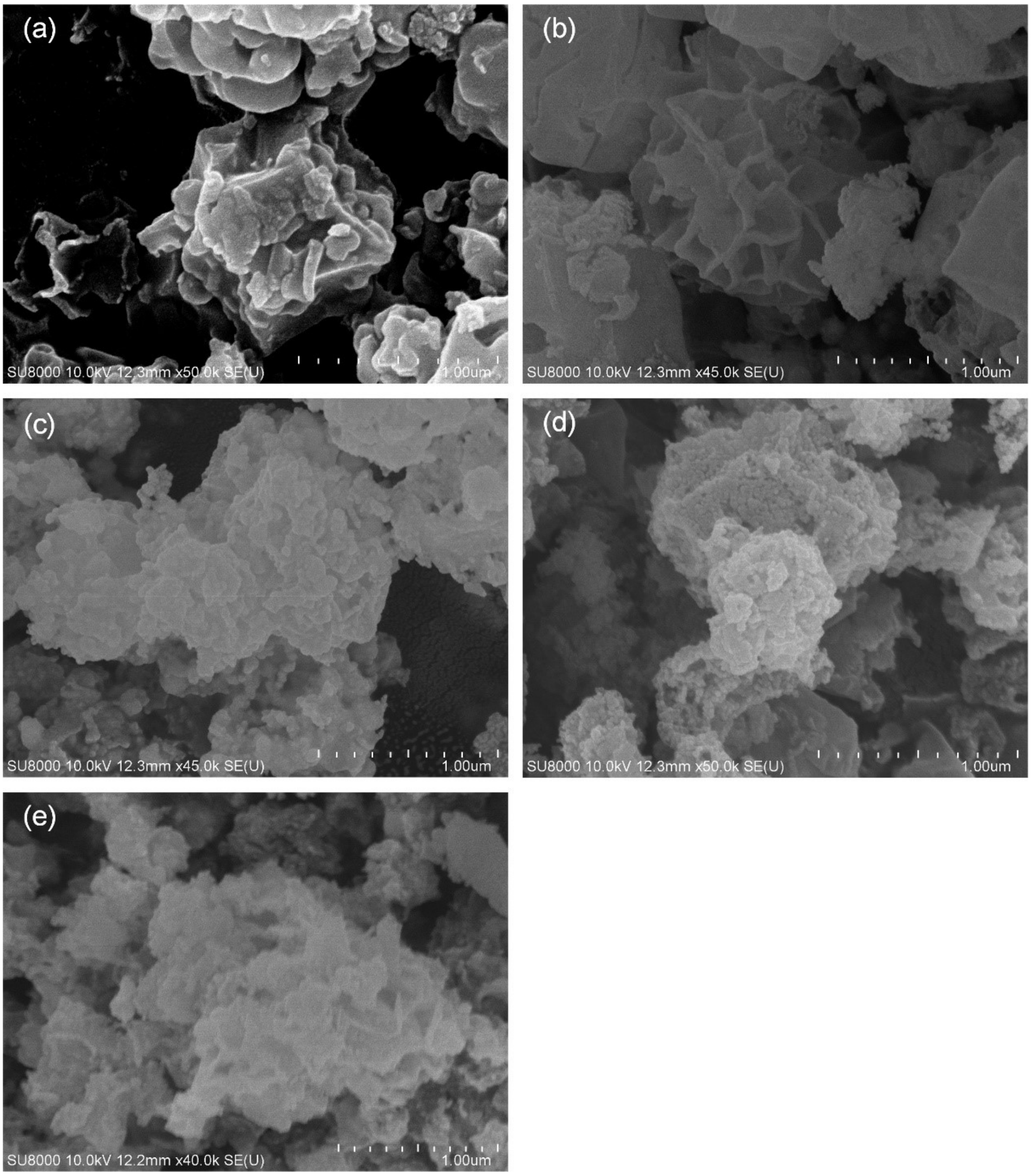

Fig. S3. SEM images of (a) Ni-CoP-300, (b) Ni-CoP-350, (c) Ni-CoP-400, (d) Ni-CoP-450 and (e) Ni-CoP-500.

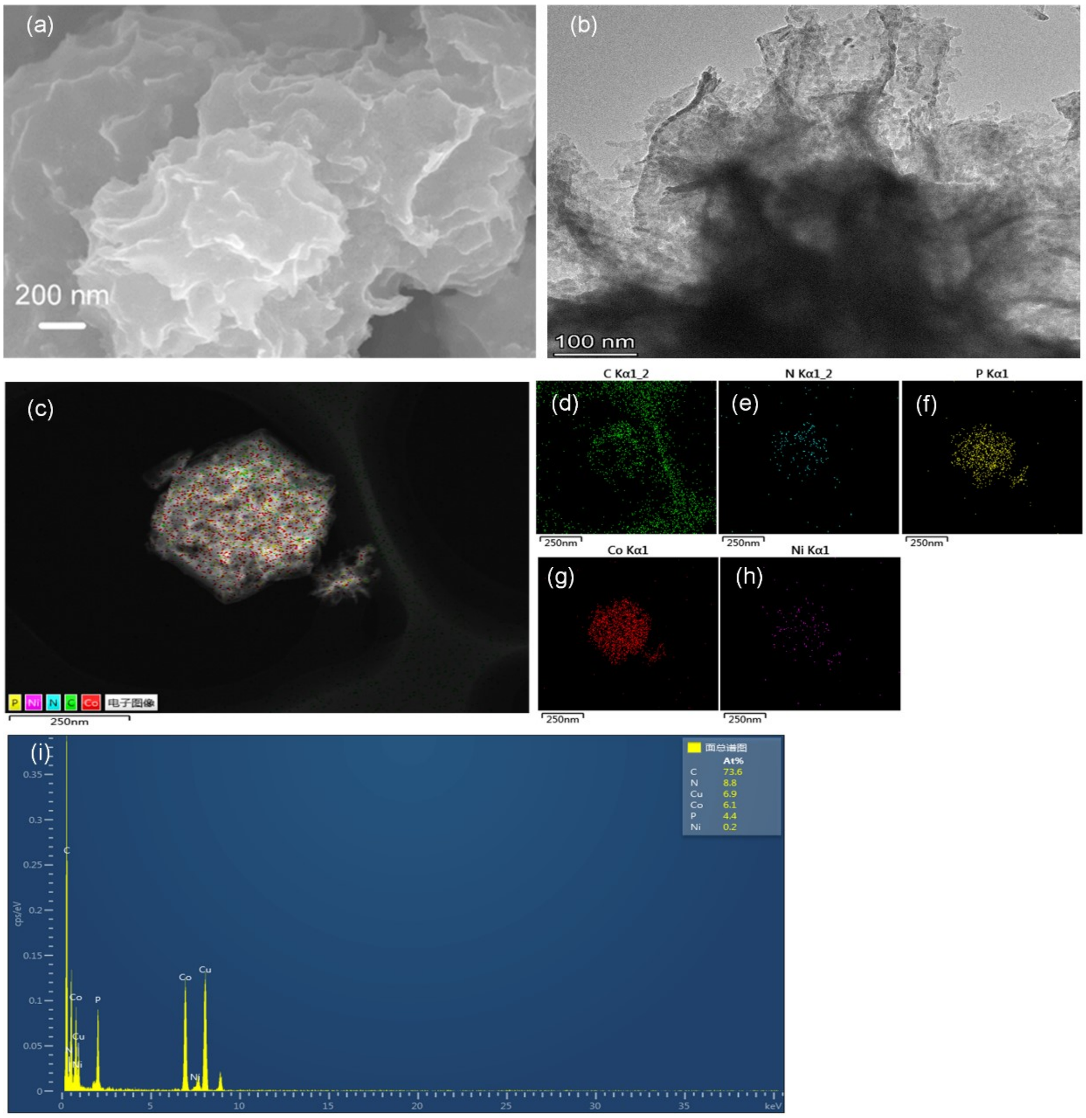

Fig. S4. (a) FESEM and (b) TEM images of the Ni-CoP-350, (c) the EDS mappings of the Ni-CoP-350. (d-h) EDS mapping of C, N, P, Co and Ni obtained from the area in (c), (h) The content ratio of each element in Ni-CoP-350.

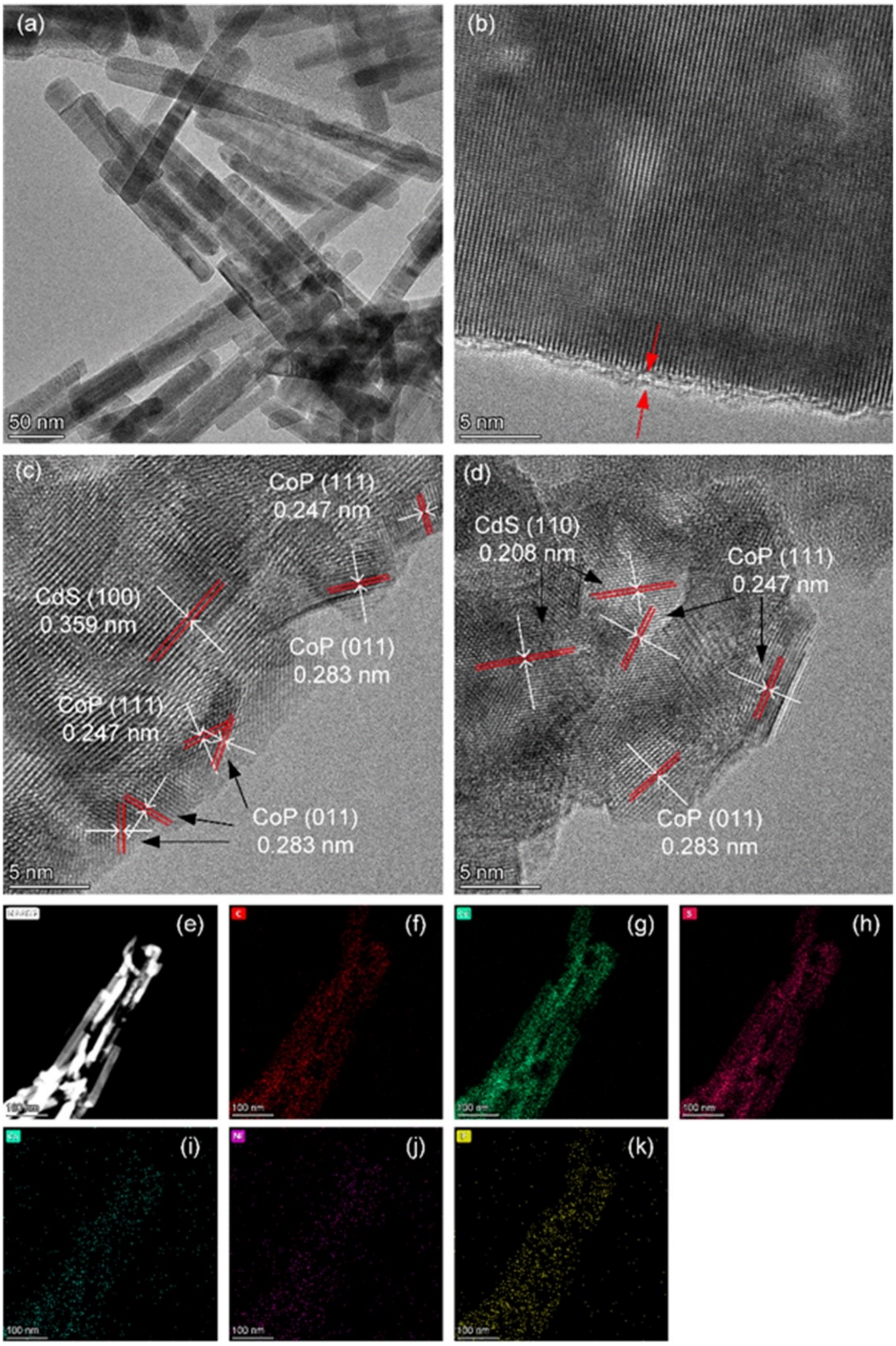

Fig. S5. (a) TEM and (b-d) HRTEM images, (e) HAADF-STEM image and (f-k) the corresponding EDS mappings of the 7% Ni-CoP/CdS photocatalyst.

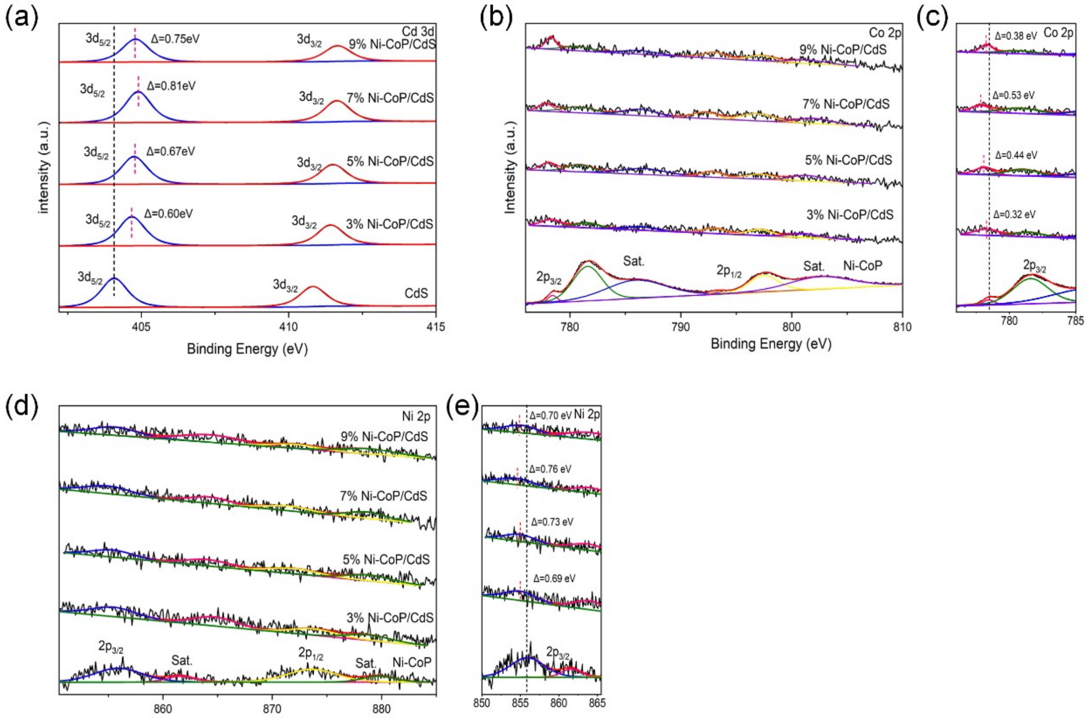

Fig. S6. High-resolution XPS spectra of (a) Cd 3d, (b) Co 2p, (c) Partial enlargement view of Co 2p, (d) Ni 2p, (e) Partial enlargement view of Ni 2p of the as-prepared x% Ni-CoP/CdS and Ni-CoP. (x=3, 5, 7, and 9)

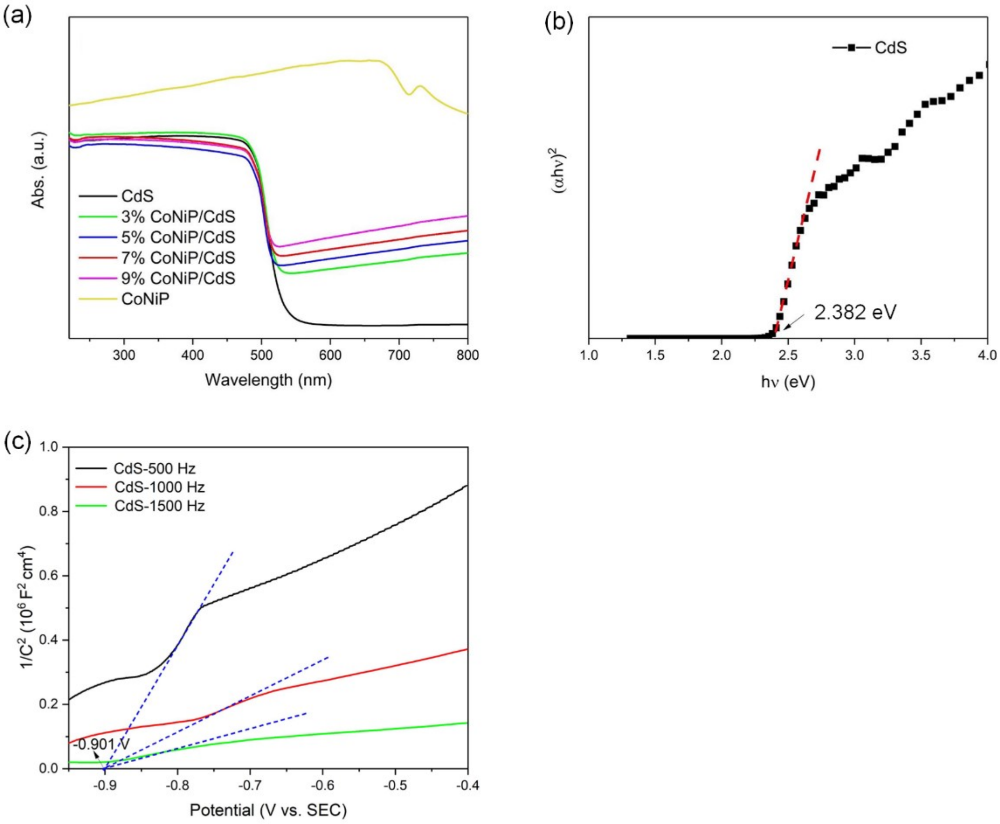

Fig. S7. (a) UV-vis diffuse reflectance spectra of the samples, (b) Tauc plots of CdS, (c) Mott–Schottky plots of CdS measured at different frequencies of 500, 1000 and 1500 Hz.

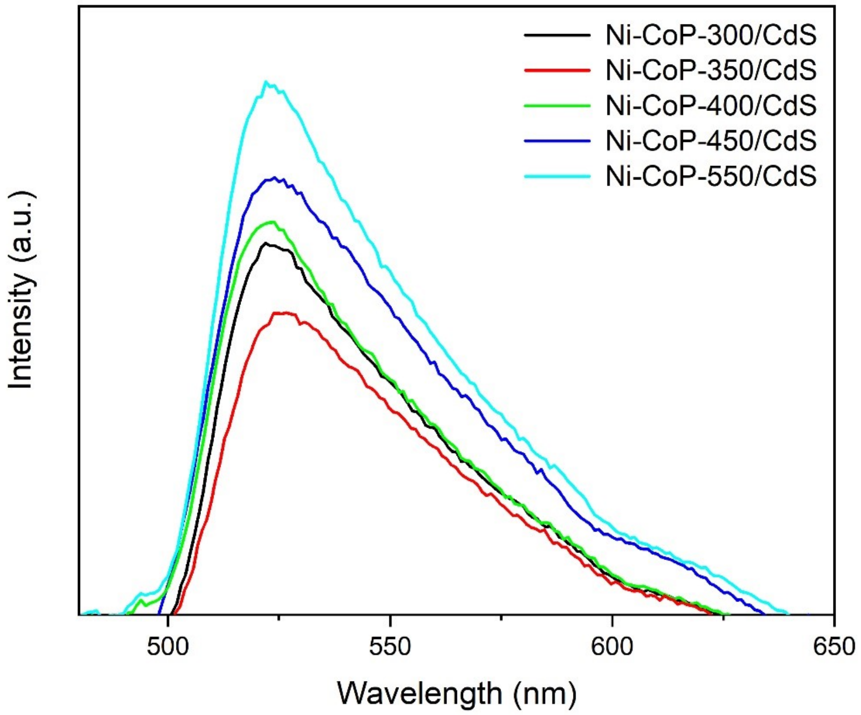

Fig. S8. Steady-state photoluminescence (PL) spectra of samples with different temperature of Ni-CoP. And the ratio of Ni-CoP with different temperature and CdS is 7%.

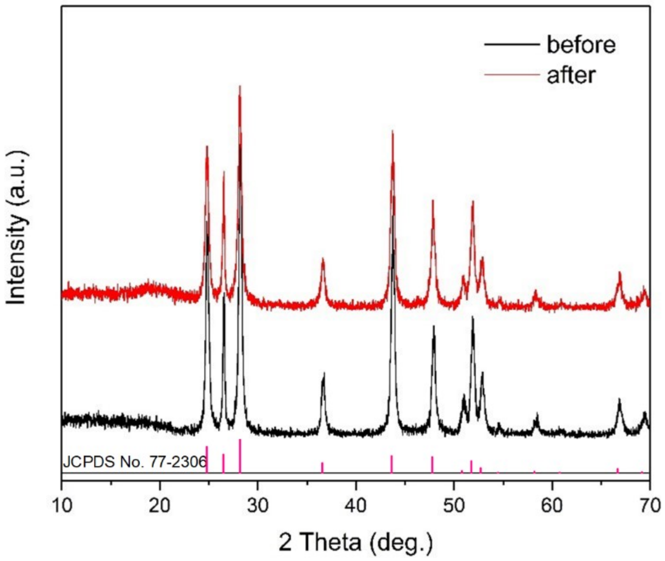

Fig. S9. XRD patterns of the 7% Ni-CoP/CdS photocatalyst before and after stability test of photocatalytic H_2 production under visible light irradiation.

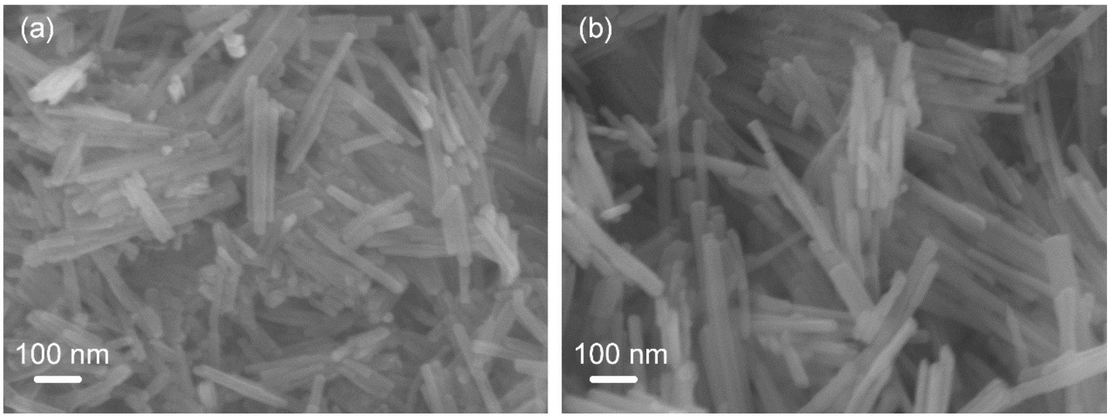

Fig. S10. FESEM images of the 7% Ni-CoP/CdS photocatalyst before (a) and after (b) stability test of photocatalytic H_2 production under visible light irradiation.

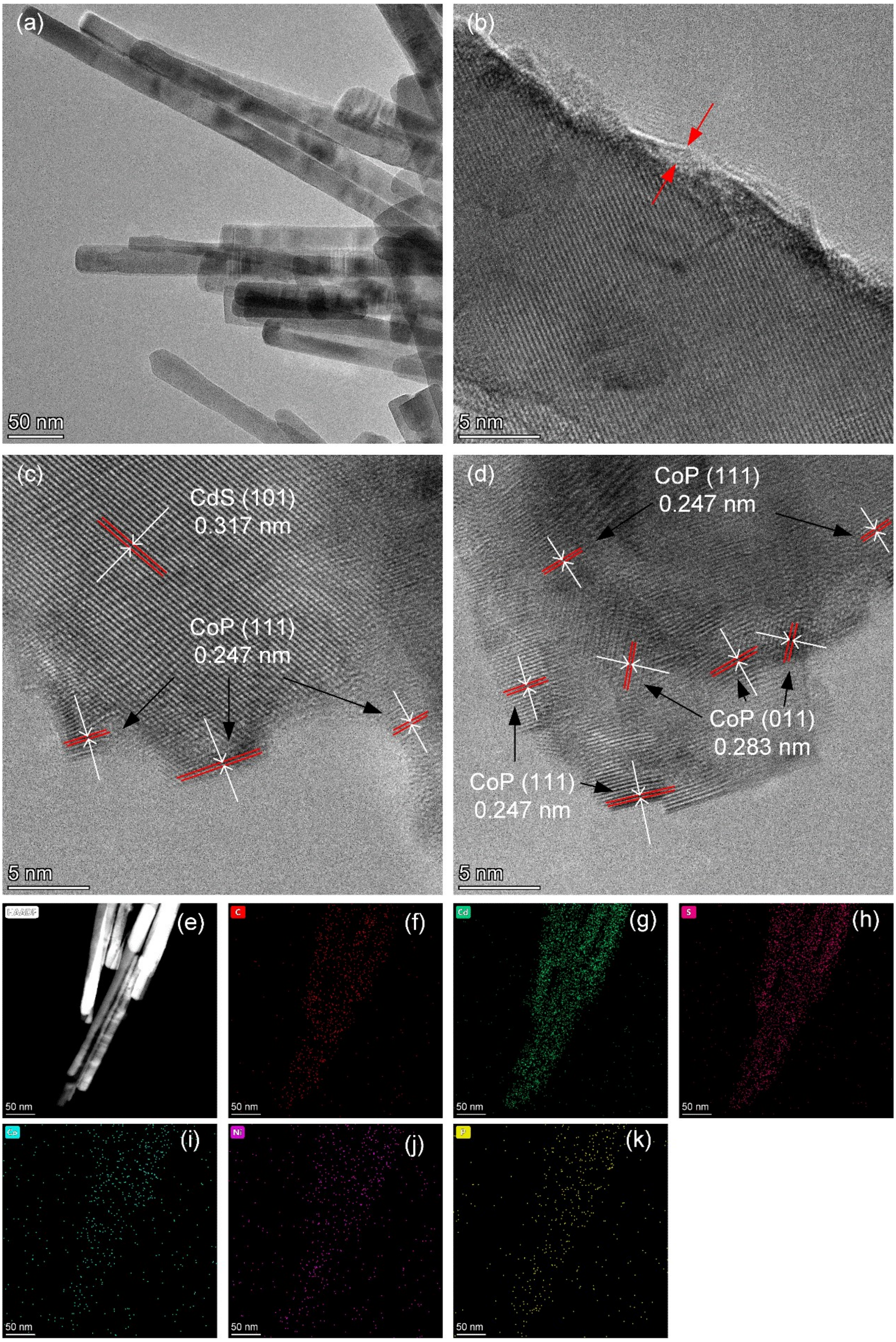

Fig. S11. (a-d) TEM and HRTEM images, HAADF-STEM image (e) and the corresponding EDS mappings (f-k) of the 7% Ni-CoP/CdS photocatalyst after stability test of photocatalytic H_2 production under visible light irradiation.

Table S1. Photocatalytic hydrogen production has been reported in the literature.

Catalysts	Hydrogen production rate (umol/h/g)	Hydrogen production rate of CdS (umol/h/g)	stability	References
7% Ni-CoP/CdS	28357	1873	no obvious decrease	This work
CdS–$ZnO_{0.5}$	805.5	66.9	slightly decrease	[1]
0.75% wtPt/CdS	13000	2400	slightly decrease	[2]
10.3% CdS@Zn-C	6600	1400	no obvious decrease	[3]
CdS/Ag_2S/NiS	48280	1030	decrease	[4]
CdS-10% $Ti_3C_2T_x$	15400	4800	no obvious decrease	[5]
C-ZnO/CdS-4	20250	830	decrease	[6]
Au@HCS@PdS	16350	146	no obvious decrease	[7]

Table S2. Zeta potential of the CdS and Ni-CoP

Sample	CdS	Ni-CoP
Zeta potential (mV)	-25.5	+ 52.4

1. G. Sun, B. Xiao, H. Zheng, J.-W. Shi, S. Mao, C. He, Z. Li and Y. Cheng, *Journal of Materials Chemistry A*, 2021, **9**, 9735-9744.
2. X. Lu, A. Tong, D. Luo, F. Jiang, J. Wei, Y. Huang, Z. Jiang, Z. Lu and Y. Ni, *Journal of Materials Chemistry A*, 2022, **10**, 4594-4600.
3. Y. Shi, X. Lei, L. Xia, Q. Wu and W. Yao, *Chemical Engineering Journal*, 2020, **393**.
4. B. He, C. Bie, X. Fei, B. Cheng, J. Yu, W. Ho, A. A. Al-Ghamdi and S. Wageh, *Applied Catalysis B: Environmental*, 2021, **288**, 119994.
5. J.-Y. Li, Y.-H. Li, F. Zhang, Z.-R. Tang and Y.-J. Xu, *Applied Catalysis B: Environmental*, 2020, **269**.
6. S. Liang, G. Sui, J. Li, D. Guo, Z. Luo, R. Xu, H. Yao, C. Wang and S. Chen, *International Journal of Hydrogen Energy*, 2022, **47**, 11190-11202.
7. X.-l. Li, G.-q. Yang, S.-s. Li, N. Xiao, N. Li, Y.-q. Gao, D. Lv and L. Ge, *Chemical Engineering Journal*, 2020, **379**, 122350.